

Electronic energy levels in semiconductor nanocrystals: A Wannier function approach

Ari Mizel and Marvin L. Cohen

*Department of Physics, University of California at Berkeley, Berkeley, California 94720
and Materials Science Division, Lawrence Berkeley National Laboratory, Berkeley, California 94720*

(Received 10 January 1997; revised manuscript received 3 April 1997)

We present a flexible and computationally efficient scheme for calculating electronic eigenstates of semiconductor nanocrystals using Wannier functions. With this method, we compute the band gap of CdS nanocrystals and compare our calculations with experiment. This approach also enables us to study the dependence of the gap on nanocrystal shape. By investigating spherical, cubical, and tetrahedral nanocrystals, we show that the gap is sensitive to the total number of atoms in a nanocrystal but not to their arrangement. Our theoretical analysis gives justification and clarification to the band-structure discretization method. [S0163-1829(97)01035-7]

I. INTRODUCTION

The size-dependent properties of semiconductor nanocrystals have attracted considerable interest from physicists and chemists both because of the scientific questions they raise and because of their potential technological applications.¹ As the investigation of size-dependent properties progresses, experimental techniques for nanocrystal synthesis and analysis continue to improve.² At the same time, theoretical methods for computing nanocrystal properties develop increasing accuracy.

Past theoretical studies of electronic and structural properties have included effective mass calculations, tight binding calculations, band-structure discretization, and other approaches.^{3–11} Such varied schemes have been suggested because semiconductor nanocrystals are in a difficult size regime: they are generally too big for molecular techniques but too small for a bulk computation that ignores the nanocrystal surface.⁸

We present here a Wannier function method for determining the electronic spectra of nanocrystals. The technique is simple, flexible, and computationally undemanding. It requires no effective mass approximation of parabolic energy bands, which can lead to an exaggeration of nanocrystal band gaps.⁶ It is applicable to nanocrystals of arbitrary shape, which is important given the variety of experimental geometries and the shape restrictions of some previous methods.^{3–5,9} Also, this method treats the conduction band as accurately as the valence bands, in contrast to tight binding calculations.⁶

As an application of the Wannier function technique, we compute the band gap of CdS nanocrystals and show that the results agree with recent measurements within experimental uncertainty. Then we investigate theoretically the dependence of the band gap upon nanocrystal shape. We find that the band gap depends strongly upon the number of unit cells in the nanocrystal but only weakly upon their arrangement.

II. METHOD

The Wannier function approach provides a means of calculating the electronic properties of a large nanocrystal given

the electronic properties of the bulk crystal. Suppose that the bulk crystal has a single particle Hamiltonian

$$H_{\text{bulk}} = \frac{p^2}{2m_e} + U_{\text{bulk}}(\vec{r}) \quad (1)$$

with eigensolution

$$H_{\text{bulk}}\psi_{n,\vec{k}}(\vec{r}) = E_n(\vec{k})\psi_{n,\vec{k}}(\vec{r}). \quad (2)$$

We define Wannier functions, in terms of Bloch wave functions, by

$$a_n(\vec{r}-\vec{R}) \equiv \frac{1}{\sqrt{\Omega}} \int_{\text{BZ}} d^3k e^{-i\vec{k}\cdot\vec{R}} \psi_{n,\vec{k}}(\vec{r}), \quad (3)$$

where \vec{R} is a lattice vector, Ω is the volume of the first Brillouin zone (BZ), and the integral proceeds over the BZ. These Wannier functions provide an orthonormal basis, $\int a_n^*(\vec{r}-\vec{R}_i) a_m(\vec{r}-\vec{R}_j) d^3r = \delta_{mn} \delta_{ij}$, and they have the important characteristic that $a_n(\vec{r}-\vec{R})$ is localized about the lattice site \vec{R} (see Appendix). These properties suggest the use of Wannier functions as orbitals in tight binding style calculations. To obtain the interaction integral between any two Wannier orbitals, we combine Eqs. (2) and (3) to find

$$\begin{aligned} \langle a_{n,\vec{R}_i} | H_{\text{bulk}} | a_{m,\vec{R}_j} \rangle &= \int a_n^*(\vec{r}-\vec{R}_i) H_{\text{bulk}} a_m(\vec{r}-\vec{R}_j) d^3r \\ &= \delta_{mn} \widetilde{E}_n(\vec{R}_i - \vec{R}_j). \end{aligned} \quad (4)$$

In this equation

$$\widetilde{E}_n(\vec{R}) \equiv \frac{1}{\Omega} \int_{\text{BZ}} d^3k e^{i\vec{k}\cdot\vec{R}} E_n(\vec{k}) \quad (5)$$

is a sort of Fourier component of the bulk band structure.

Given the interaction integrals (4), we are in a position to make tight binding style calculations for nanocrystals as follows. If we imagine choosing a fragment of the bulk crystal and clearing away the other atoms, the Hamiltonian of the remaining “nanocrystal” is

$$H_{\text{nano}} = \frac{p^2}{2m_e} + U_{\text{nano}} = H_{\text{bulk}} + (U_{\text{nano}} - U_{\text{bulk}}). \quad (6)$$

If the surface of the nanocrystal is passivated with organic ligands or other adsorbates, as in experimentally realized nanocrystals,^{1,2,12} then the energy difference $U_{\text{nano}}(\vec{r}) - U_{\text{bulk}}(\vec{r})$ should be small inside the nanocrystal and large outside. In this paper, we assume that

$$U_{\text{nano}}(\vec{r}) - U_{\text{bulk}}(\vec{r}) \approx \begin{cases} 0 & \vec{r} \text{ inside} \\ \infty & \vec{r} \text{ outside.} \end{cases} \quad (7)$$

Now we find that for \vec{R}_i and \vec{R}_j inside the nanocrystal, the interaction matrix element is

$$\begin{aligned} \langle a_{n,\vec{R}_i} | H_{\text{nano}} | a_{m,\vec{R}_j} \rangle &\equiv \int d^3 r a_n^*(\vec{r} - \vec{R}_i) [H_{\text{bulk}} + (U_{\text{nano}} - U_{\text{bulk}})] a_m(\vec{r} - \vec{R}_j) \\ &\approx \int d^3 r a_n^*(\vec{r} - \vec{R}_i) H_{\text{bulk}} a_m(\vec{r} - \vec{R}_j) \\ &= \delta_{mn} \tilde{E}_n(\vec{R}_i - \vec{R}_j), \end{aligned} \quad (8)$$

where we have used the fact that $a_n(\vec{r} - \vec{R}_i)$ and $a_m(\vec{r} - \vec{R}_j)$ are both localized inside the nanocrystal. For \vec{R}_i outside the nanocrystal,

$$\begin{aligned} \langle a_{n,\vec{R}_i} | H_{\text{nano}} | a_{m,\vec{R}_i} \rangle &\equiv \int d^3 r a_n^*(\vec{r} - \vec{R}_i) [H_{\text{bulk}} + (U_{\text{nano}} \\ &\quad - U_{\text{bulk}})] a_m(\vec{r} - \vec{R}_i) \approx \delta_{m,n} \infty. \end{aligned} \quad (9)$$

Thus, the low energy eigenvectors of the matrix $\langle a_{n,\vec{R}_i} | H_{\text{nano}} | a_{m,\vec{R}_j} \rangle$ will involve no contribution from any $a_n(\vec{r} - \vec{R})$ for which \vec{R} is outside the nanocrystal. We can therefore approximate the eigenstates and eigenvalues of H_{nano} by simply diagonalizing the matrix

$$\langle a_{n,\vec{R}_i} | H_{\text{nano}} | a_{m,\vec{R}_j} \rangle \approx \delta_{m,n} \tilde{E}_n(\vec{R}_i - \vec{R}_j) \quad (10)$$

for \vec{R}_i and \vec{R}_j restricted to the nanocrystal interior.

This is the Wannier function approach employed in this paper. It is related to the tight binding approximation, but it possesses several advantages. First, it includes the interaction matrix elements between any two orbitals, nearest neighbors, and beyond. Second, the bulk conduction band is modeled no less accurately than the bulk valence band. Finally, since the Wannier functions have a precise relationship to the Bloch functions, it is possible to use them to demonstrate trends relating the electronic energy spectrum of a nanocrystal to that of the bulk crystal, as we show in Sec. IV.

The Wannier function approach should be valid provided that the nanocrystal is large enough for approximation (7) to hold. If a very small nanocrystal were to possess significant deviations from the bulk lattice structure, the method would become inapplicable.

We apply this method to CdS nanocrystals in the zinc-blende lattice structure. The bulk band structure $E_n(\vec{k})$ is computed using an empirical pseudopotential method¹³ in a

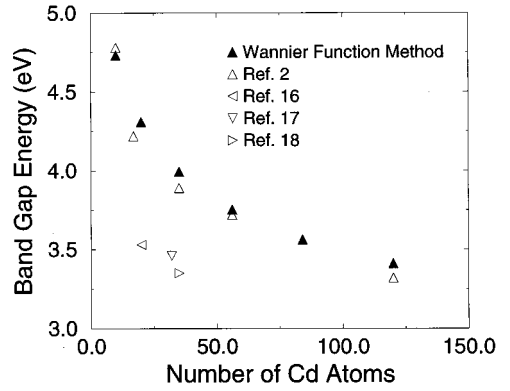


FIG. 1. Comparison between Wannier function method and experiment for zinc-blende CdS nanocrystal gaps. Note that the exciton binding energy is not included in the theoretical computation. The experimental points are given in Table I.

basis of 169 plane waves. This basis size is sufficient to converge $E_n(\vec{k})$ to better than 0.01 eV. The empirical pseudopotential gives a zinc-blende CdS energy gap of 2.44 eV, which is 0.06 eV smaller than the experimental gap. For the nanocrystal calculations here, we determine $E_n(\vec{k})$ at 2856 k points throughout the irreducible part of the first Brillouin zone, which is sufficient to provide a well-converged evaluation of Eq. (5).

Approximate eigenvalues and eigenstates of the nanocrystal are obtained for each “band” n by diagonalizing the matrix $\langle a_{n,\vec{R}_i} | H_{\text{nano}} | a_{n,\vec{R}_j} \rangle \approx \tilde{E}_n(\vec{R}_i - \vec{R}_j)$, where \vec{R}_i and \vec{R}_j are kept within the nanocrystal. The band gap energy is obtained by subtracting the largest eigenvalue of the matrix $\langle a_{v,\vec{R}_i} | H_{\text{nano}} | a_{v,\vec{R}_j} \rangle$, where v denotes the valence band, from the smallest eigenvalue of $\langle a_{c,\vec{R}_i} | H_{\text{nano}} | a_{c,\vec{R}_j} \rangle$, and where c denotes the conduction band. It is convenient from a computational standpoint that, if only the band gap is desired, we need never perform a full diagonalization of $\langle a_{v,\vec{R}_i} | H_{\text{nano}} | a_{v,\vec{R}_j} \rangle$ and $\langle a_{c,\vec{R}_i} | H_{\text{nano}} | a_{c,\vec{R}_j} \rangle$ but rather may simply find the appropriate extreme eigenvalues.

III. COMPUTATIONAL RESULTS

Our numerical computations of CdS nanocrystal band gaps are shown in Fig. 1. Experiments suggest that small CdS nanocrystals favor a tetrahedral shape,^{2,12} so our calculations are for tetrahedral nanocrystals with various numbers of cadmium atoms. Comparison between theory and experiment is difficult, because experimentalists quote exciton energy (band gap minus exciton binding energy) as a function of nanocrystal radius, but it is not obvious how to interpret the radius measurements. For instance, Wang and Herron¹² assign a 10 Å diameter to a nanocrystal with 20 Cd atoms and a 3.53 eV exciton energy, while Vossmeier and co-workers² measure a diameter of 12.8 Å for a nanocrystal of ~ 10 Cd atoms and a 4.78 eV exciton energy. Such differences arise for at least two reasons. First, the diameter of a tetrahedral nanocrystal can be defined in more than one way (e.g., Wang and Herron report the base to tip distance of the $\text{Cd}_{13}\text{S}_{13}$ core of their nanocrystal, whereas the radius measured by Vossmeier and co-workers may include some

TABLE I. Experimental data points used in Fig. 1. Nanocrystals in the experimental literature with the radii too large to permit an accurate estimate of N were omitted from the comparison. Nanocrystals known to possess a wurtzite structure were also omitted.

Ref.	Reported radius (Å)	E_{ex} (eV)	N	Estimation method
2	6.4	4.78	10	Experimentalist's suggestion
2	7.2	4.22	17	Experimentalist's suggestion
2	8.0	3.89	35	Tetrahedron with $N > 17$, $N < 56$
2	9.3–10	3.72	56	six lattice planes in TEM image
2	11.6–13	3.32	120	eight lattice planes in TEM image
16	5	3.53	20	Experimentalist's suggestion
17	7.5	3.46	32	Structure known
18	13	3.35	35	Experimentalist's suggestion

portion of the surface ligands). Second, experimentalists use different organic ligands, of different sizes, to passivate the surfaces of their nanocrystals. These ligands can affect the size measurements, particularly for small nanocrystals.²

Because of the difficulty in interpreting the radius measurements, we compare our calculations with experiment by estimating the number, N , of Cd atoms in each experimental nanocrystal. In many cases, experimentalists have given a suggestion for N for a given nanocrystal sample or know the structure well enough to specify N exactly. For other cases, we must estimate N by assuming that the nanocrystal is a tetrahedron and using a measurement of the number of lattice planes. Some experimental nanocrystals were too large to permit an accurate estimate of N ; we omitted these from our comparison. For completeness, in Table I, we list each experimental point with a measured radius, a measured exciton energy, an estimate for the value of N , and the method used to make this estimate.

It should be emphasized that the Wannier function method produces the band gap without a correction for the exciton binding energy present in the experimental measurements. To account for this Coulomb energy, most previous researchers have utilized a formula

$$E_{\text{Coul}} = -\frac{1.8e^2}{\epsilon R}, \quad (11)$$

where R is the nanocrystal radius. This formula is based upon a effective mass study of an electron and a hole in a spherical cavity.⁴ In order to make use of it, we would have to find the appropriate R for each experimental nanocrystal, which is difficult as mentioned above. Furthermore, recent pseudopotential calculations¹¹ suggest that formula (11) substantially overestimates the Coulomb energy. Thus, we omit from our calculations the correction (11). Regardless of this correction, our results appear to fall within the uncertainty in the experimental data.

Figure 2 shows the gap versus the number of unit cells in the nanocrystal for a variety of nanocrystal shapes. The plot indicates that the band gap depends mainly on the number of unit cells and not very strongly upon the shape into which those cells are arranged. This result has also been found in studies of Si quantum dots.¹⁰ The finding suggests that it is inappropriate to model a tetrahedron shaped nanocrystal with a sphere of the same general radius, since the sphere would have many more unit cells.

IV. RELATIONSHIP BETWEEN NANOCRYSTAL AND BULK EIGENSPECTRA

In addition to our computational results, we present here analytical arguments for how the eigenspectrum changes as a function of nanocrystal size. First of all, as the nanocrystal grows in size, within our model the band gap cannot increase. We see this in the following way. The valence band Hamiltonian matrix, $\langle a_{v,\vec{R}_i} | H_{\text{nano}} | a_{v,\vec{R}_j} \rangle$, simply acquires additional rows and columns as the nanocrystal grows to include more and more \vec{R}_i inside. But, when one adds a row and a column to a Hermitian matrix, the largest eigenvalue of the matrix can never decrease. This is because the largest eigenvector of the original matrix can be used to place a variational lower bound on the largest eigenvalue of the expanded matrix. Thus, the largest eigenvalue of the valence band Hamiltonian matrix can never decrease as the nanocrystal grows, and, similarly, the smallest eigenvalue of the conduction band Hamiltonian can never increase as the nanocrystal grows. So, as the nanocrystal grows, the band gap cannot increase.

We now make a quantitative approximation to the band gap of a nanocrystal of $N_1 \times N_2 \times N_3$ unit cells. First, we observe that the Hamiltonian matrix $\langle a_{n,\vec{R}_i} | H_{\text{nano}} | a_{n,\vec{R}_j} \rangle \approx \tilde{E}_n(\vec{R}_i - \vec{R}_j)$ is a kind of Toeplitz matrix, which is a matrix T with the property that the value of $T_{i,j}$ depends only upon the difference of its indices $T_{i,j} = T(i-j)$.¹⁴ Given this ob-

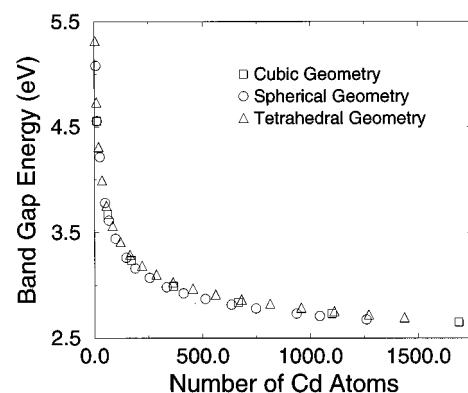


FIG. 2. Calculated band gaps for various nanocrystal shapes. The gaps depend strongly upon the number of Cd atoms in the nanocrystal, but only weakly upon the shape.

servation, we apply a theorem on the extreme eigenvalues of Toeplitz forms¹⁴ to approximate the small eigenvalues of the Hamiltonian matrix by

$$E_n \left[\vec{k}_{\min} + \pi \left(\frac{p}{N_1} \hat{b}_1 + \frac{q}{N_2} \hat{b}_2 + \frac{r}{N_3} \hat{b}_3 \right) \right], \quad (12)$$

where \hat{b}_i are unit reciprocal lattice vectors, p, q, r are positive integers, and the bulk band structure $E_n(\vec{k})$ has a minimum at \vec{k}_{\min} . A similar result holds for the large eigenvalues of the Hamiltonian matrix, with \vec{k}_{\min} replaced by \vec{k}_{\max} . Thus, it follows that the band gap of a nanocrystal with $N_1 \times N_2 \times N_3$ unit cells is approximately

$$E_g \approx E_c \left[\vec{k}_{\min} + \pi \left(\frac{1}{N_1} \hat{b}_1 + \frac{1}{N_2} \hat{b}_2 + \frac{1}{N_3} \hat{b}_3 \right) \right] - E_v \left[\vec{k}_{\max} + \pi \left(\frac{1}{N_1} \hat{b}_1 + \frac{1}{N_2} \hat{b}_2 + \frac{1}{N_3} \hat{b}_3 \right) \right], \quad (13)$$

where c denotes the conduction band and v denotes the valence band. This reduces in the effective mass approximation to the result

$$E_g \approx E_g(\text{bulk}) + \frac{\hbar^2 \pi^2}{2m_c} \left(\frac{1}{N_1^2} + \frac{1}{N_2^2} + \frac{1}{N_3^2} \right) - \frac{\hbar^2 \pi^2}{2m_v} \left(\frac{1}{N_1^2} + \frac{1}{N_2^2} + \frac{1}{N_3^2} \right), \quad (14)$$

which should be accurate for large N_1 , N_2 , and N_3 . Equations (12)–(14) are useful because they provide some intuition about the behavior of the eigenspectrum as a function of nanocrystal size and further justify the method of calculating nanocrystal eigenspectra by band-structure discretization.⁹

Strictly speaking, Eq. (12) is based on a theorem of Toeplitz forms which need not apply to our matrix $\langle a_{n,\vec{R}_i} | H_{\text{nano}} | a_{n,\vec{R}_j} \rangle \approx \tilde{E}_n(\vec{R}_i - \vec{R}_j)$, since it depends upon the three components of the vector $\vec{R}_i - \vec{R}_j$, rather than upon a single difference $i - j$. However, it is possible to justify Eq. (12) rigorously when the band structure separates into a sum of functions of the components of \vec{k} , $E_n(\vec{k}) = E_{n,1}(k_1) + E_{n,2}(k_2) + E_{n,3}(k_3)$, as in the effective mass approximation. For then, Eq. (5) shows that $\tilde{E}_n(\vec{R}_i - \vec{R}_j)$ decouples into a sum of Toeplitz matrices,

$$\begin{aligned} \tilde{E}_n(\vec{R}_i - \vec{R}_j) &= \delta_{R_{i,2}, R_{j,2}} \delta_{R_{i,3}, R_{j,3}} \tilde{E}_{n,1}(R_{i,1} - R_{j,1}) \\ &\quad + \delta_{R_{i,3}, R_{j,3}} \delta_{R_{i,1}, R_{j,1}} \tilde{E}_{n,2}(R_{i,2} - R_{j,2}) \\ &\quad + \delta_{R_{i,1}, R_{j,1}} \delta_{R_{i,2}, R_{j,2}} \tilde{E}_{n,3}(R_{i,3} - R_{j,3}), \end{aligned} \quad (15)$$

where $R_{i,1}$ is the first component of \vec{R}_i , etc, and the Toeplitz form theorem can be applied iteratively to obtain Eq. (12).

V. CONCLUSION

In conclusion, we find that the Wannier function method provides a flexible and computationally inexpensive ap-

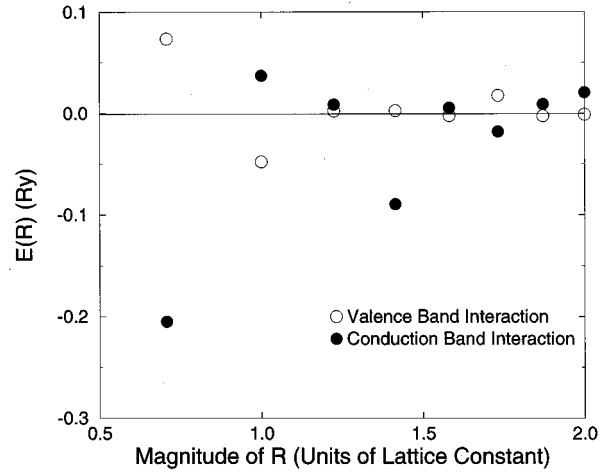


FIG. 3. Interaction matrix elements between Wannier functions. In the valence band, interactions are negligible beyond second nearest neighbors. In the conduction band, interactions are negligible beyond fourth nearest neighbors.

proach to the nanocrystal electronic eigenproblem. It successfully reproduces experimental gaps in CdS nanocrystals, and it shows that, for relatively round shapes, the gap depends strongly upon number of unit cells but only weakly upon the arrangement of those unit cells. This method should be particularly well suited for computations of the density of states and may be appropriate for calculations of higher electronic transitions and other electronic properties.

ACKNOWLEDGMENTS

This work was supported by National Science Foundation Grant No. DMR-9520554, and the Director, Office of Energy Research, Office of Basic Energy Services, Materials Sciences Division of the U.S. Department of Energy under Contract No. DE-AC03-76SF00098. A.M. acknowledges the support of the National Science Foundation. We would like to express our gratitude to Jeffrey C. Grossman for his insightful suggestions and for his critical reading of the manuscript. We would also like to thank Michel Côté and Vincent H. Crespi for several stimulating discussions.

APPENDIX

That Wannier functions are localized in space is well known. However, the degree of localization is a subtle question. For an isolated band, localization can be optimized by carefully choosing the phase of the Bloch functions $\psi_{n,\vec{k}}$ in Eq. (3). However, this choice is irrelevant to our calculations since the phase of $\psi_{n,\vec{k}}$ does not effect the Hamiltonian matrix elements in Eq. (10).

For bands with degeneracies, the localization of the Wannier functions can suffer. To address this concern, we plotted the interaction matrix elements (5) for the conduction band and the valence band in CdS. Figure 3 shows that interac-

tions between valence band Wannier functions are negligible beyond second nearest neighbors, while interactions between conduction band Wannier functions are negligible beyond fourth nearest neighbors. It is possible, but nontrivial, to re-

define the Wannier functions to improve localization in the presence of band degeneracies. However, we did not make such an effort since it is unlikely to improve significantly upon the calculations presented here. See Ref. 15 for details.

-
- ¹A. P. Alivasaos, *Science* **271**, 933 (1996).
- ²T. Vossmeyer *et al.*, *J. Phys. Chem.* **98**, 7665 (1994).
- ³Al. L. Efros and A. L. Efros, *Fiz. Tekh. Poluprovodn.* **16**, 1209 (1982) [*Sov. Phys. Semicond.* **16**, 772 (1982)].
- ⁴L. E. Brus, *J. Chem. Phys.* **80**, 4403 (1984).
- ⁵A. I. Ekimov, F. Hache, M. C. Schanne-Klein, D. Ricard, C. Flytzanis, I. A. Kudryavtsev, T. V. Yazeva, A. V. Rodina, and Al. L. Efros, *J. Opt. Soc. Am. B* **10**, 100 (1993).
- ⁶P. E. Lippens and M. Lannoo, *Phys. Rev. B* **41**, 6079 (1990); **39**, 10 935 (1989).
- ⁷L. M. Ramaniah and S. V. Nair, *Phys. Rev. B* **47**, 7132 (1993).
- ⁸N. A. Hill and K. B. Whaley, *J. Chem. Phys.* **99**, 3707 (1993).
- ⁹A. Tomasulo and M. V. Ramakrishna, *J. Chem. Phys.* **105**, 3612 (1996); B. Zorman, M. V. Ramakrishna, and R. A. Friesner, *J. Phys. Chem.* **99**, 7649 (1995); M. V. Rama Krishna and R. A. Friesner, *Phys. Rev. Lett.* **67**, 629 (1991); *J. Chem. Phys.* **95**, 8309 (1991).
- ¹⁰L. Wang and A. Zunger, *Phys. Rev. B* **53**, 9579 (1996); L. Wang, *ibid.* **49**, 10 154 (1994); L. Wang and A. Zunger, *J. Chem. Phys.* **100**, 2394 (1994); L. Wang and A. Zunger, *J. Phys. Chem.* **98**, 2158 (1994).
- ¹¹A. Franceschetti and A. Zunger, *Phys. Rev. Lett.* **78**, 915 (1997).
- ¹²Ying Wang and Norman Herron, *Phys. Rev. B* **42**, 7253 (1990).
- ¹³T. K. Bergstresser and M. L. Cohen, *Phys. Rev.* **164**, 1069 (1967).
- ¹⁴U. Grenander and Gabor Szegö, *Toeplitz Forms and Their Applications* (Chelsea, New York, 1984), Chap. 5.
- ¹⁵E. I. Blount, in *Solid State Physics: Advances in Research and Applications*, edited by F. Seitz and D. Turnbull (Academic, New York, 1962), Vol. 13, p. 305.
- ¹⁶N. Herron, A. Suna, and Y. Wang, *J. Chem. Soc. Dalton Trans.* **1992**, 2329.
- ¹⁷N. Herron, J. C. Calabrese, W. E. Farneth, and Y. Wang, *Science* **259**, 1426 (1993).
- ¹⁸Y. Wang, M. Harmer, and N. Herron, *Isr. J. Chem.* **33**, 31 (1993).